Single-dose replicating RNA vaccine induces neutralizing antibodies against SARS-CoV-2 in nonhuman primates

Jesse H. Erasmus[1,2], Amit P. Khandhar[2, 3], Alexandra C. Walls[6], Emily A. Hemann[5,8], Megan A. O'Connor[1,7], Patience Murapa[1], Jacob Archer[1,3], Shanna Leventhal[4], Jim Fuller[1], Thomas Lewis[1,7], Kevin E. Draves[1], Samantha Randall[3], Kathryn A. Guerriero[7], Malcolm S. Duthie[2], Darrick Carter[2,3,5], Steven G. Reed[3,5] David W. Hawman[4], Heinz Feldmann[4], Michael Gale, Jr.[5,7,8], David Veesler[6], Peter Berglund[2], Deborah Heydenburg Fuller[1,5,7]*.

[1]Department of Microbiology, University of Washington, Seattle, WA

[2]Host Directed Therapeutics (HDT) Bio Corp, Seattle, WA

[3]PAI Life Sciences, Seattle, WA

[4]Laboratory of Virology, Division of Intramural Research, National Institute of Allergy and Infectious Diseases, National Institutes of Health, Hamilton, MT

[5]Center for Innate Immunity and Immune Disease, University of Washington, Seattle, WA

[6]Department of Biochemistry, University of Washington, Seattle, WA

[7]Washington National Primate Research Center, Seattle, WA

[8]Department of Immunology, University of Washington, Seattle, WA

*Corresponding author:

Deborah Heydenburg Fuller

Professor, Department of Microbiology, University of Washington, Seattle, WA

Division Chief, Infectious Diseases and Translational Medicine, Washington National Research Primate Research Center, Seattle, WA

fullerdh@uw.edu

Running title: Replicating RNA Vaccine for COVID-19

Keywords for submission: coronavirus; SARS-CoV-2; vaccine; RNA; replicon; nanoparticle; nonhuman primates.
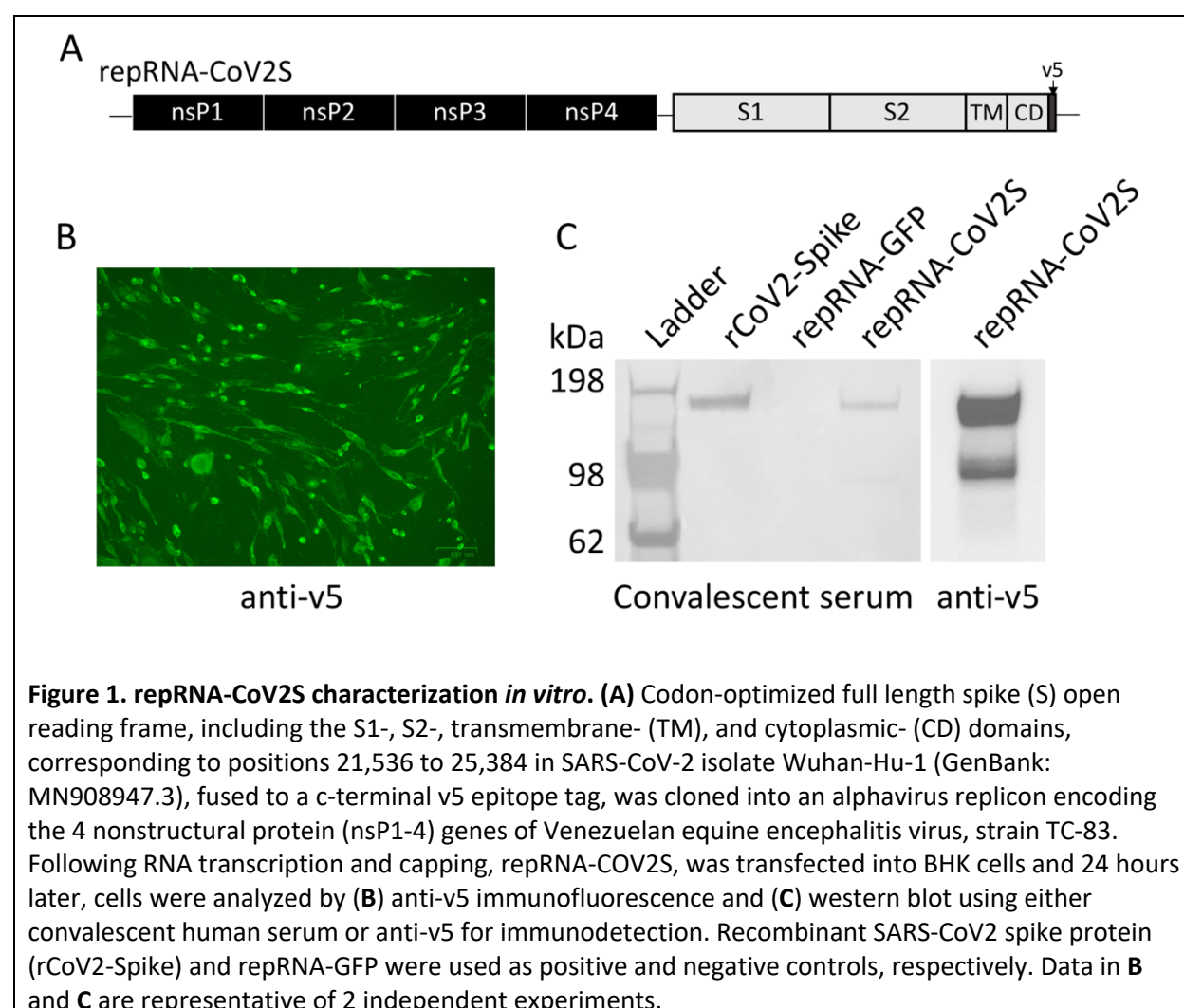
1

1 **Abstract**

2   The ongoing COVID-19 pandemic, caused by infection with SARS-CoV-2, is having a dramatic and

3 deleterious impact on health services and the global economy. Grim public health statistics highlight the

4 need for vaccines that can rapidly confer protection after a single dose and be manufactured using

5 components suitable for scale-up and efficient distribution. In response, we have rapidly developed

6 repRNA-CoV2S, a stable and highly immunogenic vaccine candidate comprised of an RNA replicon

7 formulated with a novel Lipid InOrganic Nanoparticle (LION) designed to enhance vaccine stability,

8 delivery and immunogenicity. We show that intramuscular injection of LION/repRNA-CoV2S elicits

9 robust anti-SARS-CoV-2 spike protein IgG antibody isotypes indicative of a Type 1 T helper response as

10 well as potent T cell responses in mice. Importantly, a single-dose administration in nonhuman primates

11 elicited antibody responses that potently neutralized SARS-CoV-2. These data support further

12 development of LION/repRNA-CoV2S as a vaccine candidate for prophylactic protection from SARS-CoV-
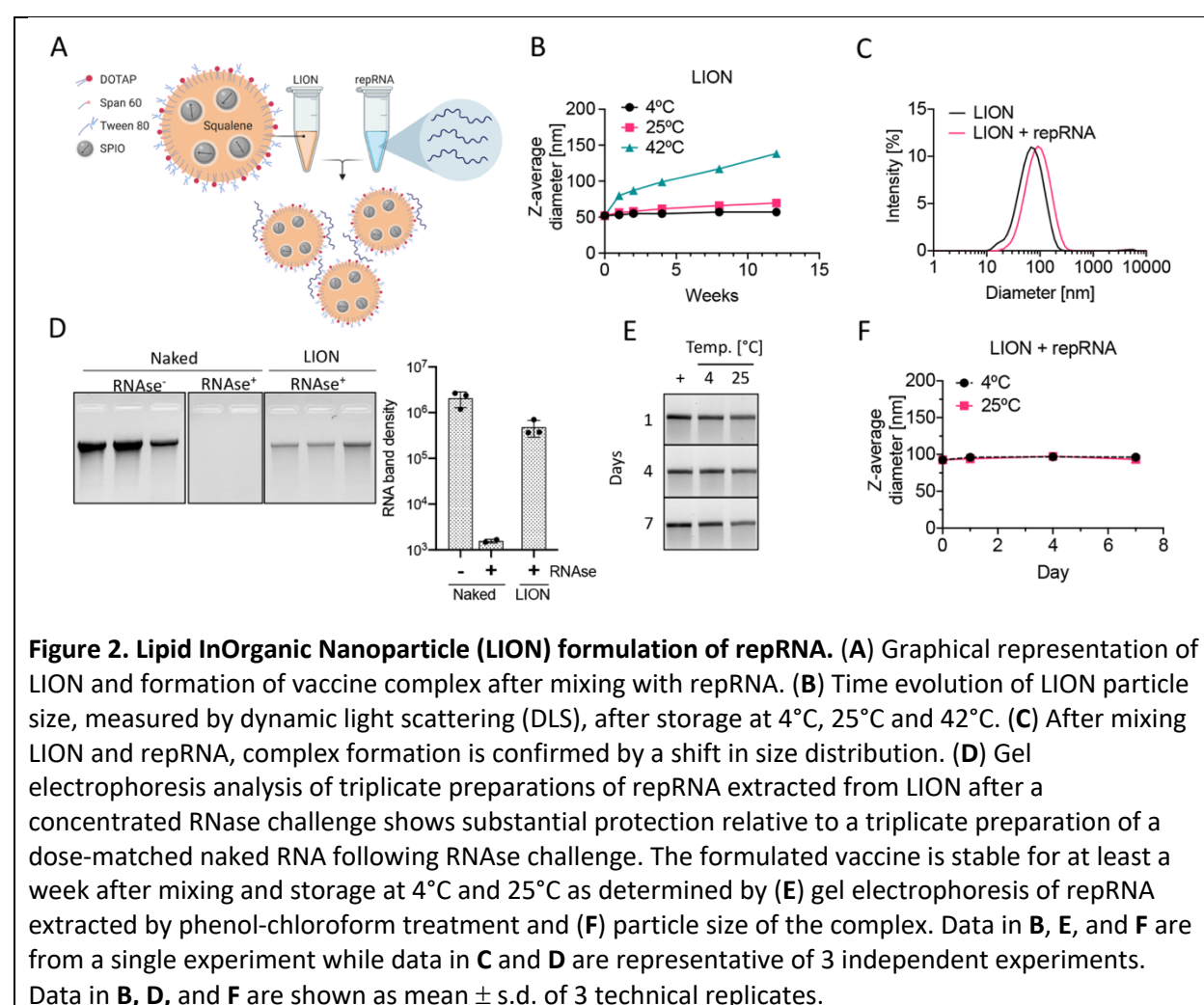
13 2 infection.

14   Severe acute respiratory syndrome coronavirus-2 (SARS-CoV-2) first emerged in December 2019

15   and within 3 months, Coronavirus Disease 2019 (COVID-19), caused by SARS-CoV-2 infection, was

16   declared a worldwide pandemic [1–3]. Coronaviruses are enveloped, single-strand positive-sense RNA

17   viruses with a large genome and open reading frames for four major structural proteins: Spike (S),

18   envelope, membrane, and nucleocapsid. The S protein mediates binding of coronaviruses to angiotensin

19   converting enzyme 2 (ACE2) on the surface of various cell types including epithelial cells of

20   the pulmonary alveolus [4–6]. Protection is thought to be mediated by neutralizing antibodies against the S

21   protein [7,8], as most of the experimental vaccines developed against the related SARS-CoV incorporated

22   the S protein, or its receptor binding domain (RBD), with the goal of inducing robust, neutralizing

23   responses [9–11]. Indeed, previous reports have shown that human neutralizing antibodies protected mice

24   challenged with SARS-CoV [12–14] and Middle East respiratory syndrome (MERS)-CoV [15] suggesting that

25   protection against SARS-CoV-2 can be mediated through anti-S antibodies. Additionally, SARS vaccines

26   that drive Type 2 T helper (Th2) responses have been associated with enhanced lung immunopathology

27   following challenge with SARS-CoV while those with a Type 1 T helper (Th1)-biased immune response

28   are associated with enhanced protection in the absence of immunopathology [16,17]. Therefore, an

29   effective COVID-19 vaccine will likely need to induce, at the very least, Th1-biased immune responses

30   comprised of SARS-CoV-2-specific neutralizing antibodies.

31   Nucleic acid vaccines have emerged as ideal modalities for rapid vaccine design, requiring only

32   the target antigen's gene sequence and removing dependence on pathogen culture (inactivated or live

33   attenuated vaccines) or scaled recombinant protein production. In addition, nucleic acid vaccines avoid

34   pre-existing immunity that can dampen immunogenicity of viral vectored vaccines. Recently, clinical

35   trials were initiated with messenger RNA (mRNA) vaccines formulated with lipid nanoparticles (LNPs)

36   and a DNA vaccine delivered by electroporation [18]. However, mRNA and DNA vaccines may not be able

37   to induce protective efficacy in humans after a single immunization since, similar to inactivated and

38   recombinant subunit protein vaccines, they typically require multiple administrations over an extended

39   period of time to become effective [19]. Virus-derived replicon RNA (repRNA) vaccines were first described

40   in 1989 and have been delivered in the forms of virus-like RNA particles (VRP), *in-vitro* transcribed (IVT)

41   RNA, and plasmid DNA [20–23]. In repRNA the open reading frame encoding the viral RNA polymerase

42   complex (most commonly from the *Alphavirus* genus) is intact but the structural protein genes are

43   replaced with an antigen-encoding gene [20,24–26]. While conventional mRNA vaccines, like that initiated in

44   a recent clinical trial, are translated directly from the incoming RNA molecules, introduction of repRNA

45   into cells initiates ongoing biosynthesis of antigen-encoding RNA that results in dramatically increased

3

46   expression and duration that significantly enhances humoral and cellular immune responses [27]. In

47   addition, repRNA vaccines mimic an alphavirus infection in that viral-sensing stress factors are triggered

48   and innate pathways are activated through Toll-like receptors and retinoic acid inducible gene (RIG)-I to

49   produce interferons, pro-inflammatory factors and chemotaxis of antigen-presenting cells, as well as

50   promoting antigen cross-priming [28]. As a result, repRNA acts as its own adjuvant, eliciting more robust

51   immune responses after a single dose, relative to conventional mRNA which typically requires multiple

52   and 1,000-fold higher doses [29]. An effective vaccine to stop a pandemic outbreak like COVID-19 would

53   ideally induce protective levels of immunity rapidly and after only a single dose while simultaneously

54   reducing the load on manufacturing at scale, due to a requirement for fewer and lower doses. Since

55   repRNA vaccines often require only a single administration to be effective [30], they offer considerable

56   potential to meet this need.

Figure 1. repRNA-CoV2S characterization *in vitro*. (A) Codon-optimized full length spike (S) open reading frame, including the S1-, S2-, transmembrane- (TM), and cytoplasmic- (CD) domains, corresponding to positions 21,536 to 25,384 in SARS-CoV-2 isolate Wuhan-Hu-1 (GenBank: MN908947.3), fused to a c-terminal v5 epitope tag, was cloned into an alphavirus replicon encoding the 4 nonstructural protein (nsP1-4) genes of Venezuelan equine encephalitis virus, strain TC-83. Following RNA transcription and capping, repRNA-COV2S, was transfected into BHK cells and 24 hours later, cells were analyzed by (**B**) anti-v5 immunofluorescence and (**C**) western blot using either convalescent human serum or anti-v5 for immunodetection. Recombinant SARS-CoV2 spike protein (rCoV2-Spike) and repRNA-GFP were used as positive and negative controls, respectively. Data in **B** and **C** are representative of 2 independent experiments.

57

58   Building on experience with the attenuated Venezuelan equine encephalitis virus (VEEV) TC-83

59   strain [22,30–34], we generated repRNAs incorporating sequences from the SARS-CoV-2 Spike (S) protein,

60   including full length S (repRNA-CoV2S) (Fig. 1A). Using immunofluorescence and western blot we

61   demonstrated efficient expression of the v5-tagged S protein in BHK cells (Fig. 1B,C). Then, utilizing

62   convalescent serum collected 29 days after onset of COVID-19 as an immunodetection reagent, we

63   demonstrated endogenous expression of an S protein in BHK cells, reactive with natural SARS-CoV-2

64   immune sera (Fig. 1C). Next, we evaluated the ability of repRNA-CoV2S to rapidly generate antibody and

65   T cell responses in mice when formulated with a novel Lipid InOrgainc Nanoparticle (LION) designed to

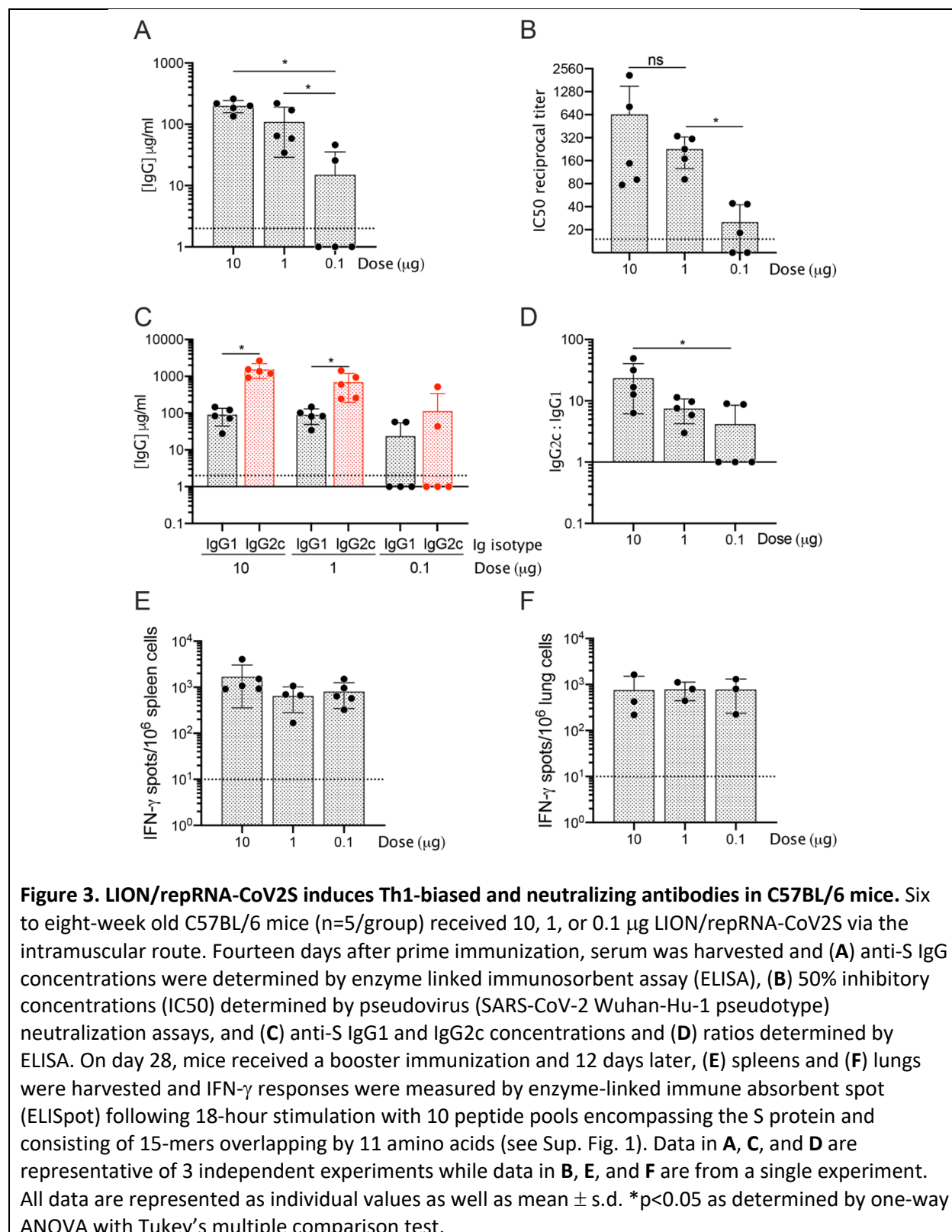66   enhance vaccine stability and intracellular delivery of the vaccine.

Figure 2. Lipid InOrganic Nanoparticle (LION) formulation of repRNA. (**A**) Graphical representation of LION and formation of vaccine complex after mixing with repRNA. (**B**) Time evolution of LION particle size, measured by dynamic light scattering (DLS), after storage at 4°C, 25°C and 42°C. (**C**) After mixing LION and repRNA, complex formation is confirmed by a shift in size distribution. (**D**) Gel electrophoresis analysis of triplicate preparations of repRNA extracted from LION after a concentrated RNase challenge shows substantial protection relative to a triplicate preparation of a dose-matched naked RNA following RNAse challenge. The formulated vaccine is stable for at least a week after mixing and storage at 4°C and 25°C as determined by (**E**) gel electrophoresis of repRNA extracted by phenol-chloroform treatment and (**F**) particle size of the complex. Data in **B**, **E**, and **F** are from a single experiment while data in **C** and **D** are representative of 3 independent experiments. Data in **B, D,** and **F** are shown as mean ± s.d. of 3 technical replicates.

67

68   LION is a highly stable cationic squalene emulsion with 15 nm superparamagnetic iron oxide

69   (Fe_3O_4) nanoparticles (SPIO) embedded in the hydrophobic oil phase. Squalene is a known vaccine

70   adjuvant [35,36] and SPIO nanoparticles have a long history of clinical use in MRI contrast and intravenous
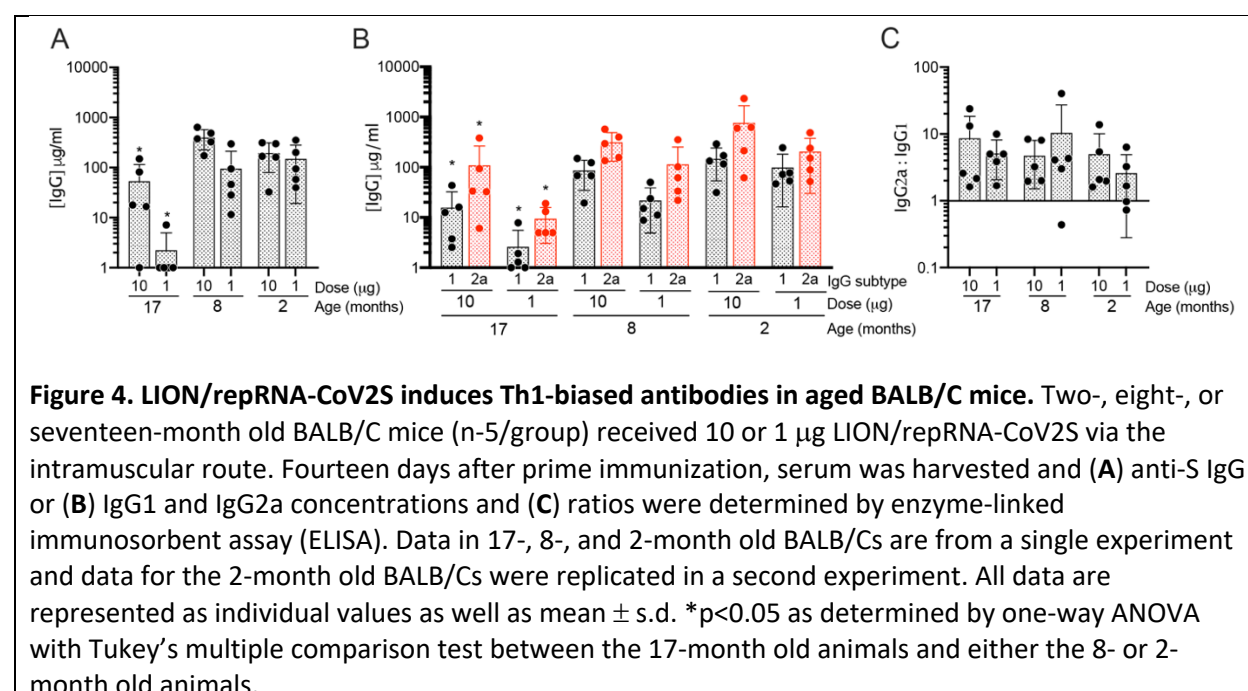
5

71   iron replacement therapy; the unique nonlinear magnetic properties of SPIOs have also been leveraged

72   for novel use in a range of imaging, targeting and therapy applications [37–42]. A key component of LION is

73   the cationic lipid 1,2-dioleoyl-3-trimethylammonium propane (DOTAP), which enables electrostatic

74   association with RNA molecules when combined by a simple 1:1 (v/v) mixing step (Fig. 2A). LION has an

75   intensity-weighted average diameter of 52 nm (PDI = 0.2) measured by dynamic light scattering (DLS).

76   The formulation is colloidally stable for at least 3 months when stored at 4 and 25°C (Fig. 2B). When

77   mixed, electrostatic association between anionic repRNA and cationic DOTAP molecules on the surface

78   of LION promotes immediate complex formation, as confirmed by increase in particle size to an

79   intensity-weighted average diameter of 90 nm detected by DLS (Fig. 2C). Gel electrophoresis analysis of

80   LION-formulated repRNA molecules extracted by phenol-chloroform treatment after a concentrated

81   RNase challenge showed substantial protection from RNase-catalyzed degradation compared to

82   unformulated repRNA (Fig. 2D). To evaluate short-term stability of the vaccine, we evaluated repRNA

83   integrity and complex stability on 1, 4 and 7 days after mixing. LION maintained full integrity of the

84   repRNA molecules (Fig. 2E) and complex size (Fig. 2F) at all time points.

85   A single intramuscular immunization of C57BL/6 mice with 10 or 1 µg of LION/repRNA-CoV2S

86   induced 100% seroconversion by 14 days post-immunization and robust anti-S IgG levels with mean

87   binding titers of 200 and 109 µg/ml, respectively, and partial seroconversion (2 out of 5) at a 0.1 µg dose

88   (Fig. 3A). Both the 10 and 1 µg prime-only doses induced neutralizing antibodies with mean 50%

89   inhibitory concentrations (IC50) of 1:643 and 1:226, respectively, as measured by pseudovirus

90   neutralization assay (SARS-CoV-2 Wuhan-Hu-1 pseudotype). While all doses induced Th1-biased immune

91   responses indicated by significantly higher IgG2c responses when compared to IgG1 (Fig. 3C), there was

92   a trend toward higher doses inducing even more Th1-biased responses as indicated by higher IgG2c:IgG1

93   ratios (Fig. 3D). Given the potential role for T cells to contribute to protection, as seen with SARS and

94   MERS [43–45], especially in the presence of waning antibody and memory B cell responses, we also

95   evaluated T cell responses to LION/repRNA-CoV2S in mice. On day 28 this same cohort of mice received

96   a second immunization and 12 days later, spleens and lungs were harvested and stimulated with an

97   overlapping 15-mer peptide library of the S protein, and IFN-γ responses were measured by enzyme-

98   linked immune absorbent spot (ELISpot) assay. Mice receiving a 10, 1, and 0.1 µg prime/boost exhibited

99   robust splenic T cell responses with mean IFN-γ spots/10^6 cells of 1698, 650, and 801, respectively (Fig.

100   3E). Robust T cell responses were also detected in the lung and were similar between groups with mean

101   IFN-γ spots/10^6 cells of 756, 784, and 777, respectively (Fig. 3F). Interestingly, analysis of the specificity

102   of peptide response showed a biased response towards the S1 domain of the S protein in the spleen

103   (Sup. Fig. 1A) whereas responses in the lung were more broadly distributed between the S1 and S2
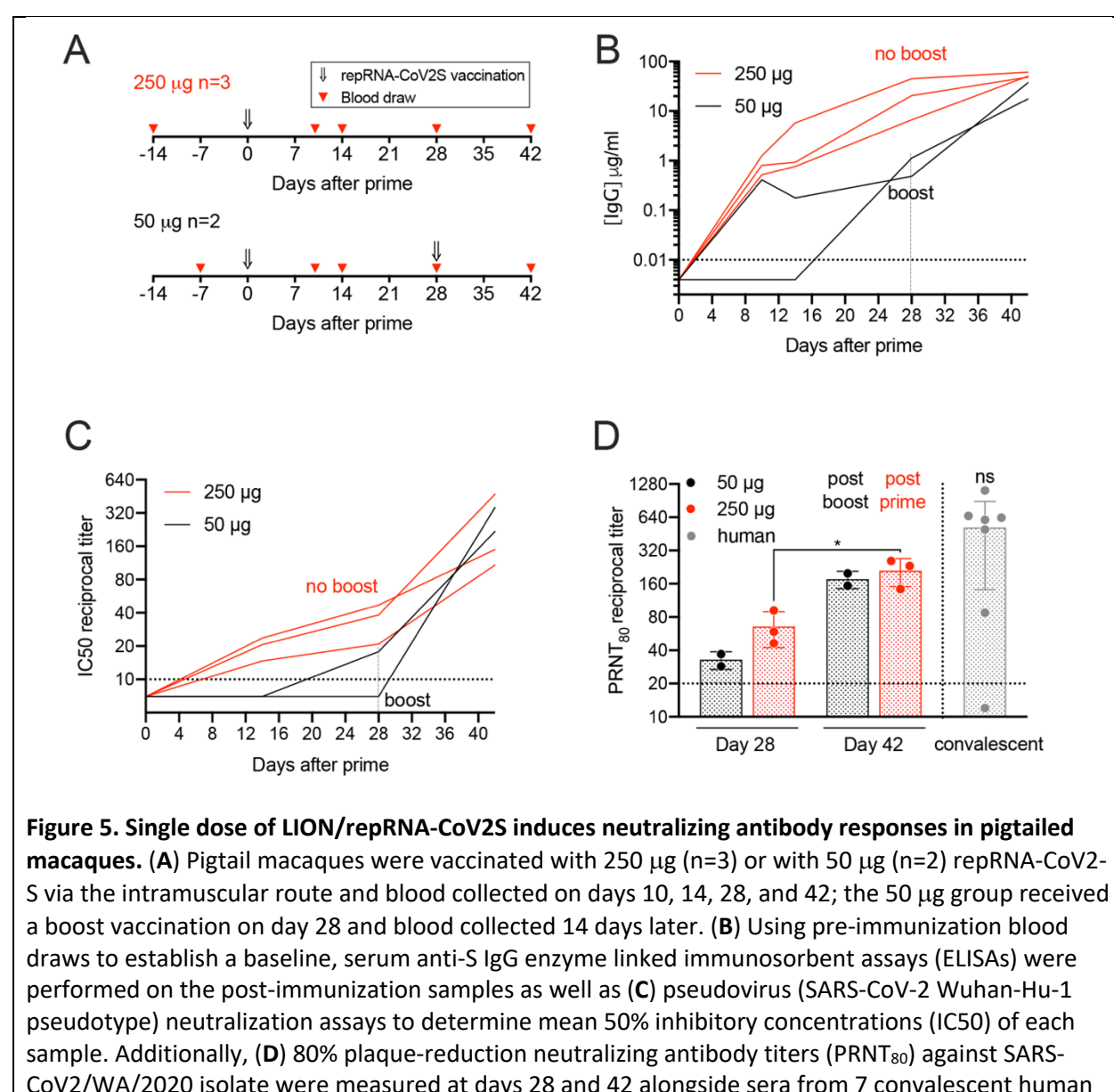
104   domains of the S protein (Sup. Fig. 1B).

Figure 3. LION/repRNA-CoV2S induces Th1-biased and neutralizing antibodies in C57BL/6 mice. Six to eight-week old C57BL/6 mice (n=5/group) received 10, 1, or 0.1 μg LION/repRNA-CoV2S via the intramuscular route. Fourteen days after prime immunization, serum was harvested and (**A**) anti-S IgG concentrations were determined by enzyme linked immunosorbent assay (ELISA), (**B**) 50% inhibitory concentrations (IC50) determined by pseudovirus (SARS-CoV-2 Wuhan-Hu-1 pseudotype) neutralization assays, and (**C**) anti-S IgG1 and IgG2c concentrations and (**D**) ratios determined by ELISA. On day 28, mice received a booster immunization and 12 days later, (**E**) spleens and (**F**) lungs were harvested and IFN-γ responses were measured by enzyme-linked immune absorbent spot (ELISpot) following 18-hour stimulation with 10 peptide pools encompassing the S protein and consisting of 15-mers overlapping by 11 amino acids (see Sup. Fig. 1). Data in **A**, **C**, and **D** are representative of 3 independent experiments while data in **B**, **E**, and **F** are from a single experiment. All data are represented as individual values as well as mean ± s.d. *p<0.05 as determined by one-way ANOVA with Tukey's multiple comparison test.

105   The elderly are among the most vulnerable to COVID-19 but immune senescence in this

106   population poses a barrier to effective vaccination. To evaluate the effect of immune senescence on

107   immunogenicity, we next administered 10 or 1 µg of LION/repRNA-CoV2S in 2-, 8-, and 17-month old

108   BALB/C mice and measured anti-S IgG concentrations at 14 days after a single immunization.

109   Significantly lower antibody titers were observed in the 17-month old mice at both doses (Fig. 4A), when

110   compared to 2- and 8-month old mice, suggesting that higher doses and/or additional booster doses

111   may be required in the most immune senescent populations to induce sufficient immunity. No

112   differences were observed between the 2- and 8-month old mice. Interestingly, although BALB/C mice

113   tend to develop a more Th2 immune-biased response following vaccination [46], LION/repRNA-CoV2S

114   induced ratios of IgG2a:IgG1 greater than 1 (Fig. 4B, C) in all age groups of BALB/C mice, indicating a

115   Th1-biased immune response. Given that severe, life-threatening COVID-19 appears to be more

116   common among elderly individuals, irrespective of type of T helper response, and that severe SARS is

117   associated with skewing toward Th2 antibody profiles with an inadequate Th1 response [16,17,43], the

118   ability of LION/repRNA-CoV2S to induce strong and Th1-biased responses in 8- and 2-month old mice,

119   even in the Th2-biased BALB/c strain, is a promising finding regarding the potential safety and

120   immunogenicity of this vaccine.

Figure 4. LION/repRNA-CoV2S induces Th1-biased antibodies in aged BALB/C mice. Two-, eight-, or seventeen-month old BALB/C mice (n-5/group) received 10 or 1 µg LION/repRNA-CoV2S via the intramuscular route. Fourteen days after prime immunization, serum was harvested and (**A**) anti-S IgG or (**B**) IgG1 and IgG2a concentrations and (**C**) ratios were determined by enzyme-linked immunosorbent assay (ELISA). Data in 17-, 8-, and 2-month old BALB/Cs are from a single experiment and data for the 2-month old BALB/Cs were replicated in a second experiment. All data are represented as individual values as well as mean ± s.d. *p<0.05 as determined by one-way ANOVA with Tukey's multiple comparison test between the 17-month old animals and either the 8- or 2-month old animals.

121

122   Having achieved robust immunogenicity with LION/repRNA-CoV2S in mice, we then immunized

123   pigtail macaques (*Macaca nemestrina*) to determine if the vaccine was capable of inducing strong

124   immune responses in a nonhuman primate model that more closely resembles humans in the immune

125   response to vaccination. Three macaques received LION/repRNA-CoV2S at a single intramuscular 250 µg

126   dose at week 0 and two macaques received a 50 µg prime at week 0 and a boost at week 4. (Fig. 5A).

127   Blood was collected 10, 14, 28, and 42 days post vaccination to monitor vaccine safety and

128   immunogenicity. There were no observed reactions at the vaccine injection site nor adverse reactions in

129   the animals up to 42 days post-prime vaccination. Additionally, there were no abnormalities in weight or

130   temperature in the animals (Sup. Fig. 2A-B), and serum chemistries revealed no abnormal findings,

131   except for mild azotemia (mildly elevated blood urea nitrogen and creatinine) in 1 animal at 14 days

132   post vaccination (Sup. Fig. 2C). All CBC counts were unremarkable (Sup. Fig. 2D).

Figure 5. Single dose of LION/repRNA-CoV2S induces neutralizing antibody responses in pigtailed macaques. (**A**) Pigtail macaques were vaccinated with 250 µg (n=3) or with 50 µg (n=2) repRNA-CoV2-S via the intramuscular route and blood collected on days 10, 14, 28, and 42; the 50 µg group received a boost vaccination on day 28 and blood collected 14 days later. (**B**) Using pre-immunization blood draws to establish a baseline, serum anti-S IgG enzyme linked immunosorbent assays (ELISAs) were performed on the post-immunization samples as well as (**C**) pseudovirus (SARS-CoV-2 Wuhan-Hu-1 pseudotype) neutralization assays to determine mean 50% inhibitory concentrations (IC50) of each sample. Additionally, (**D**) 80% plaque-reduction neutralizing antibody titers (PRNT$_{80}$) against SARS-CoV2/WA/2020 isolate were measured at days 28 and 42 alongside sera from 7 convalescent human

samples collected from confirmed COVID-19 patients (see Sup. Table 1). The experiment was performed once. Each line in **B** and **C** are representative of each individual animal. Data in **D** are reported as individual values as well as mean $\pm$ s.d. *p<0.05 as determined by students t-test comparing 250 μg groups at days 14 and 28. There was no significant difference (ns) between mean PRNT$_{80}$ titers in all 5 animals at day 42 and titers in sera from 7 convalescent humans, as measured by Mann-Whitney U test.

133

134   ELISA analyses (Sup. Fig. 3) of sera collected 10, 14, 28, and 42 days after prime immunization

135   showed that all three macaques immunized with the single 250 μg dose seroconverted as early as day

136   10, with anti-S IgG concentrations continuing to increase in these 3 animals to 48, 51, and 61 μg/ml by

137   day 42 (Fig. 5B). Both macaques receiving 50 μg repRNA-CoV2S seroconverted after a single dose but

138   developed significantly lower antibody responses with anti-S IgG concentrations of 1 and 0.5 μg/ml by

139   day 28, compared to 7, 20, and 45 μg/ml in the 250 μg group at this same time point (Fig. 5B).

140   However, 14 days after a booster immunization, the 50 μg group developed similar levels of anti-S IgG

141   concentrations (18 and 37 μg/ml) as the 250 μg prime-only group at this time point (48, 51, and 61

142   μg/ml) (Fig. 5A). Additionally, sera from the three macaques immunized with just the single 250 μg

143   dose neutralized pseudovirus (SARS-CoV-2 Wuhan-Hu-1 pseudotype) transduction of cells *in vitro* with

144   reciprocal IC50 titers of 1:38, 1:20 and 1:47 by day 28 with levels increasing to 1:472, 1:108, and 1:149

145   by day 42, whereas the 50 μg group achieved similar robust IC50 titers only after the booster

146   immunization reaching pseudovirus IC50 titers of 1:218 and 1:358 by day 42 (Fig. 5C and Sup. Fig. 4).

147   Sera collected 28- and 42-days post vaccination were further analyzed for neutralization of wild type

148   SARS-CoV-2/WA/2020 by 80% plaque reduction neutralization test (PRNT$_{80}$) and compared to

149   neutralizing titers in sera from convalescent humans collected 15-64 days following natural infection

150   (Sup. Fig. 4 and Sup. Table 1). A single immunization with 50 and 250 μg of LION/repRNA-CoV2S

151   induced mean PRNT$_{80}$ titers of 1:32 and 1:66 by day 28, respectively. By Day 42 , mean PRNT$_{80}$ titers

152   significantly increased to 1:176 after a booster immunization in the 50 μg group and to 1:211 in the

153   prime-only 250 μg group, (Fig. 5D and Sup. Fig. 4). Importantly, all 5 macaques developed PRNT$_{80}$ titers

154   within the same range as titers measured in the seven convalescent humans (<1:20 to 1:1280, collected

155   15 to 64 days post onset) and there was no significant difference in mean neutralizing titers between all

156   5 vaccinated macaques (1:197) and convalescent humans (1:518) (P=0.27, Fig. 5D, Sup. Fig. 4, and Sup.

157   Table 1). Recently, serum neutralizing titers, measured as the IC50 titer that neutralized SARS-CoV-2 by

158   50% tissue culture infectious dose (TCID$_{50}$), were reported in rhesus macaques that were either re-

159   infected [47] or challenged after vaccination with an inactivated SARS-CoV-2 vaccine [48]. In the former

160   report, IC50 titers as low as 1:8 were associated with protection from re-infection while in the latter,

10

161   IC50 titers as low as 1:50 were associated with reduced viral load and protection from lung pathology.

162   These data suggest that a 250 μg prime-only or a 50 μg prime/boost immunization with the

163   LION/repRNA-CoV2 vaccine may be able to induce levels of neutralizing antibodies sufficient to protect

164   nonhuman primates from infection and disease. Studies are now underway to evaluate protective

165   efficacy.

166   RepRNA vaccines against a variety of infectious diseases and cancers have been shown to be

167   safe and potent in clinical trials [49–52], and the cell-free and potentially highly scalable manufacturing

168   process of repRNA when used with effective synthetic formulations, such as LION, present further

169   benefits over mRNA. The two-vial approach provides a significant manufacturing and distribution

170   advantage over LNP formulations that encapsulate RNA, as the vaccine can be stockpiled and combined

171   onsite as needed. Additionally, we demonstrated that LION/repRNA-CoV-2 induces robust S-specific T

172   cell responses in mice. Given the relatively recent emergence of SARS-CoV-2, we can only speculate

173   based on limited knowledge from previous reports of coronavirus infection as to how T cell responses

174   may contribute to protection from infection and disease. Following natural infection of humans with

175   the related SARS-CoV, neutralizing antibody and memory B cell responses in some individuals are

176   reported to be short lived (~ 3 years) while memory T cells persist at least 6 years [53], suggesting a

177   potential role for T cells in long term responses especially in those who lack robust memory B cell

178   responses. Additionally, anti-S T-cell responses to the related SARS- and MERS-CoVs contribute towards

179   viral clearance in normal as well as aged mice infected with SARS- or MERS-CoV, respectively [43–45].

180   Together, our results demonstrate a significant potential for LION/repRNA-CoV2S, which will

181   enter clinical development under the name HDT-301, to induce rapid immune protection from SARS-

182   CoV-2 infection. A scalable and widely-distributed vaccine capable of inducing robust immunity in both

183   young and aged populations against SARS-CoV-2 infection in a single shot would provide immediate

184   and effective containment of the pandemic. Critically, the vaccine induced Th1-biased antibody and T

185   cell responses in both young and aged mice, an attribute that has been associated with improved

186   recovery and milder disease outcomes in SARS-CoV-infected patients [54]. Together, these results support

187   further development of LION/repRNA-CoV2S as a vaccine candidate for protection from COVID19.

188

189   **Acknowledgements**

Conflict of interest statement

207   JHE, APK, JA, MD, DC, PB, MG, and SGR have equity interest in HDT Biocorp. JHE, PB, JF, DHF, HF and DH

208   are inventors on a patent filing pertaining to repRNA-CoV2S. JHE, APK, DC, MD and SGR are inventors on

209   a patent filing pertaining to LION formulation.

References

1. Lu, H., Stratton, C. W. & Tang, Y.-W. Outbreak of pneumonia of unknown etiology in Wuhan, China: The mystery and the miracle. *J. Med. Virol.* **92**, 401–402 (2020).

2. Wu, F. *et al.* A new coronavirus associated with human respiratory disease in China. *Nature* **579**, 265–269 (2020).

3. Wang, C., Horby, P. W., Hayden, F. G. & Gao, G. F. A novel coronavirus outbreak of global health concern. *Lancet (London, England)* **395**, 470–473 (2020).

4. Hamming, I. *et al.* Tissue distribution of ACE2 protein, the functional receptor for SARS coronavirus. A first step in understanding SARS pathogenesis. *J. Pathol.* **203**, 631–637 (2004).

5. Letko, M., Marzi, A. & Munster, V. Functional assessment of cell entry and receptor usage for SARS-CoV-2 and other lineage B betacoronaviruses. *Nat. Microbiol.* **5**, 562–569 (2020).

6. Walls, A. C. *et al.* Structure, Function, and Antigenicity of the SARS-CoV-2 Spike Glycoprotein. *Cell* **181**, 281-292.e6 (2020).

7. Walls, A. C. *et al.* Unexpected Receptor Functional Mimicry Elucidates Activation of Coronavirus Fusion. *Cell* **176**, 1026-1039.e15 (2019).

8. Pinto, D. *et al.* Structural and functional analysis of a potent sarbecovirus neutralizing antibody. *bioRxiv* (2020) doi:10.1101/2020.04.07.023903.

9. He, Y., Lu, H., Siddiqui, P., Zhou, Y. & Jiang, S. Receptor-binding domain of severe acute respiratory syndrome coronavirus spike protein contains multiple conformation-dependent epitopes that induce highly potent neutralizing antibodies. *J. Immunol.* **174**, 4908–4915 (2005).

10. Jiang, S., He, Y. & Liu, S. SARS vaccine development. *Emerg. Infect. Dis.* **11**, 1016–1020 (2005).

11. Du, L. *et al.* The spike protein of SARS-CoV--a target for vaccine and therapeutic development. *Nat. Rev. Microbiol.* **7**, 226–236 (2009).

12. Menachery, V. D. *et al.* SARS-like WIV1-CoV poised for human emergence. *Proc. Natl. Acad. Sci. U. S. A.* **113**, 3048–3053 (2016).

13. Rockx, B. *et al.* Structural basis for potent cross-neutralizing human monoclonal antibody protection against lethal human and zoonotic severe acute respiratory syndrome coronavirus challenge. *J. Virol.* **82**, 3220–3235 (2008).

14. Traggiai, E. *et al.* An efficient method to make human monoclonal antibodies from memory B cells: potent neutralization of SARS coronavirus. *Nat. Med.* **10**, 871–875 (2004).

15. Corti, D. *et al.* Prophylactic and postexposure efficacy of a potent human monoclonal antibody against MERS coronavirus. *Proc. Natl. Acad. Sci. U. S. A.* **112**, 10473–10478 (2015).

242 16.   Tseng, C.-T. *et al.* Immunization with SARS coronavirus vaccines leads to pulmonary

243   immunopathology on challenge with the SARS virus. *PLoS One* **7**, e35421 (2012).

244 17.   Honda-Okubo, Y. *et al.* Severe Acute Respiratory Syndrome-Associated Coronavirus Vaccines

245   Formulated with Delta Inulin Adjuvants Provide Enhanced Protection while Ameliorating Lung

246   Eosinophilic Immunopathology. *J. Virol.* **89**, 2995–3007 (2015).

247 18.   Thanh Le, T. *et al.* The COVID-19 vaccine development landscape. *Nature reviews. Drug discovery*

248   (2020) doi:10.1038/d41573-020-00073-5.

249 19.   Shang, W., Yang, Y., Rao, Y. & Rao, X. The outbreak of SARS-CoV-2 pneumonia calls for viral

250   vaccines. *npj Vaccines* **5**, 18 (2020).

251 20.   Xiong, C. *et al.* Sindbis virus: an efficient, broad host range vector for gene expression in animal

252   cells. *Science (80-.).* **243**, 1188 LP – 1191 (1989).

253 21.   Zhou, X. *et al.* Self-replicating Semliki Forest virus RNA as recombinant vaccine. *Vaccine* **12**, 1510–

254   1514 (1994).

255 22.   Ljungberg, K. & Liljeström, P. Self-replicating alphavirus RNA vaccines. *Expert Rev. Vaccines* **18**, 1-

256   18 [Epub ahead of print] (2014).

257 23.   Frolov, I. *et al.* Alphavirus-based expression vectors: strategies and applications. *Proc. Natl. Acad.*

258   *Sci.* **93**, 11371–11377 (2002).

259 24.   Bredenbeek, P. J., Frolov, I., Rice, C. M. & Schlesinger, S. Sindbis virus expression vectors:

260   packaging of RNA replicons by using defective helper RNAs. *J. Virol.* **67**, 6439–6446 (1993).

261 25.   Liljestrom, P. & Garoff, H. A new generation of animal cell expression vectors based on the

262   Semliki Forest virus replicon. *Biotechnology. (N. Y).* **9**, 1356–1361 (1991).

263 26.   Pushko, P. *et al.* Replicon-helper systems from attenuated Venezuelan equine encephalitis virus:

264   expression of heterologous genes in vitro and immunization against heterologous pathogens in

265   vivo. *Virology* **239**, 389–401 (1997).

266 27.   Berglund, P., Smerdou, C., Fleeton, M. N., Tubulekas, I. & Liljestrom, P. Enhancing immune

267   responses using suicidal DNA vaccines. *Nat. Biotechnol.* **16**, 562–565 (1998).

268 28.   Jensen, S. & Thomsen, a. R. Sensing of RNA Viruses: a Review of Innate Immune Receptors

269   Involved in Recognizing RNA Virus Invasion. *J. Virol.* **86**, 2900–2910 (2012).

270 29.   Vogel, A. B. *et al.* Self-Amplifying RNA Vaccines Give Equivalent Protection against Influenza to

271   mRNA Vaccines but at Much Lower Doses. *Mol. Ther.* **26**, 446–455 (2018).

272 30.   Strauss, J. H. & Strauss, E. G. The alphaviruses: gene expression, replication, and evolution.

273   *Microbiol. Rev.* **58**, 491–562 (1994).

274   31.   Kinney, R. M. *et al.* Attenuation of Venezuelan equine encephalitis virus strain TC-83 is encoded

275   by the 5'-noncoding region and the E2 envelope glycoprotein. *J. Virol.* **67**, 1269–1277 (1993).

276   32.   Atasheva, S. *et al.* Pseudoinfectious Venezuelan Equine Encephalitis Virus: a New Means of

277   Alphavirus Attenuation. *J. Virol.* **87**, 13 (2016).

278   33.   Erasmus, J. H. *et al.* A Nanostructured Lipid Carrier for Delivery of a Replicating Viral RNA

279   Provides Single, Low-Dose Protection against Zika. *Mol. Ther.* **26**, 1–16 (2018).

280   34.   Duthie, M. S. *et al.* Heterologous Immunization With Defined RNA and Subunit Vaccines

281   Enhances T Cell Responses That Protect Against Leishmania donovani. *Front. Immunol.* **9**, 2420

282   (2018).

283   35.   Calabro, S. *et al.* The adjuvant effect of MF59 is due to the oil-in-water emulsion formulation,

284   none of the individual components induce a comparable adjuvant effect. *Vaccine* **31**, 3363–3369

285   (2013).

286   36.   Desbien, A. L. *et al.* Squalene emulsion potentiates the adjuvant activity of the TLR4 agonist, GLA,

287   via inflammatory caspases, IL-18, and IFN-γ. *Eur. J. Immunol.* **45**, 407–417 (2015).

288   37.   Yu, E. Y. *et al.* Magnetic Particle Imaging for Highly Sensitive, Quantitative, and Safe in Vivo Gut

289   Bleed Detection in a Murine Model. *ACS Nano* **11**, 12067–12076 (2017).

290   38.   Khandhar, A. P. *et al.* Evaluation of PEG-coated iron oxide nanoparticles as blood pool tracers for

291   preclinical magnetic particle imaging. *Nanoscale* **9**, 1299–1306 (2017).

292   39.   Bauer, L. M., Situ, S. F., Griswold, M. A. & Samia, A. C. S. High-performance iron oxide

293   nanoparticles for magnetic particle imaging - guided hyperthermia (hMPI). *Nanoscale* **8**, 12162–

294   12169 (2016).

295   40.   Zhao, Y., Zhao, X., Cheng, Y., Guo, X. & Yuan, W. Iron Oxide Nanoparticles-Based Vaccine Delivery

296   for Cancer Treatment. *Mol. Pharm.* **15**, 1791–1799 (2018).

297   41.   Zanganeh, S. *et al.* Iron oxide nanoparticles inhibit tumour growth by inducing pro-inflammatory

298   macrophage polarization in tumour tissues. *Nat. Nanotechnol.* **11**, 986–994 (2016).

299   42.   Khandhar, A. P. *et al.* Evaluating size-dependent relaxivity of PEGylated-USPIOs to develop

300   gadolinium-free T1 contrast agents for vascular imaging. *J. Biomed. Mater. Res. A* **106**, 2440–

301   2447 (2018).

302   43.   Zhao, J., Zhao, J. & Perlman, S. T cell responses are required for protection from clinical disease

303   and for virus clearance in severe acute respiratory syndrome coronavirus-infected mice. *J. Virol.*

304   **84**, 9318–9325 (2010).

305   44.   Channappanavar, R., Zhao, J. & Perlman, S. T cell-mediated immune response to respiratory

15

306   coronaviruses. *Immunol. Res.* **59**, 118–128 (2014).

307   45.   Channappanavar, R., Fett, C., Zhao, J., Meyerholz, D. K. & Perlman, S. Virus-Specific Memory CD8

308   T Cells Provide Substantial Protection from Lethal Severe Acute Respiratory Syndrome

309   Coronavirus Infection. *J. Virol.* **88**, 11034–11044 (2014).

310   46.   Mills, C. D., Kincaid, K., Alt, J. M., Heilman, M. J. & Hill, A. M. M-1/M-2 Macrophages and the

311   Th1/Th2 Paradigm. *J. Immunol.* **164**, 6166–6173 (2000).

312   47.   Bao, L. *et al.* Reinfection could not occur in SARS-CoV-2 infected rhesus macaques. *bioRxiv*

313   2020.03.13.990226 (2020) doi:10.1101/2020.03.13.990226.

314   48.   Gao, Q. *et al.* Development of an inactivated vaccine candidate for SARS-CoV-2. *Science (80-.).*

315   **1932**, eabc1932 (2020).

316   49.   Bernstein, D. I. *et al.* Randomized, double-blind, Phase 1 trial of an alphavirus replicon vaccine for

317   cytomegalovirus in CMV seronegative adult volunteers. *Vaccine* **28**, 484–493 (2009).

318   50.   Hubby, B. *et al.* Development and preclinical evaluation of an alphavirus replicon vaccine for

319   influenza. *Vaccine* **25**, 8180–8189 (2007).

320   51.   Morse, M. A. *et al.* Phase I study of alphaviral vector (AVX701) in colorectal cancer patients:

321   comparison of immune responses in stage III and stage IV patients. *J. Immunother. Cancer* **3**,

322   P444–P444 (2015).

323   52.   Reap, E. A. *et al.* Development and preclinical evaluation of an alphavirus replicon particle

324   vaccine for cytomegalovirus. *Vaccine* **25**, 7441–7449 (2007).

325   53.   Tang, F. *et al.* Lack of Peripheral Memory B Cell Responses in Recovered Patients with Severe

326   Acute Respiratory Syndrome: A Six-Year Follow-Up Study. *J. Immunol.* **186**, 7264–7268 (2011).

327   54.   Li, C. K. *et al.* T Cell Responses to Whole SARS Coronavirus in Humans. *J. Immunol.* **181**, 5490–

328   5500 (2008).

329

330

16

331   **Supplementary Material**

332   **Materials and Methods**

333   ***SARS-CoV-2 repRNA vaccine production and qualification.*** Codon optimized gene sequences

334   for SARS-CoV-2 full S corresponding to positions 21,536 to 25,384 in SARS-CoV-2 isolate Wuhan-

335   Hu-1 (GenBank: MN908947.3) fused to a c-terminal v5 epitope tag was synthesized as double

336   stranded DNA fragments (IDT) and cloned into a plasmid vector encoding the 5' and 3'

337   untranslated regions as well as the nonstructural open reading frame of Venezuelan equine

338   encephalitis virus, strain TC-83, between PflFI and SacII sites by Gibson assembly (SGI-DNA).

339   Clones were then sanger sequenced and prepped for RNA production as follows. Template DNA

340   was linearized by enzymatic digestion with NotI followed by phenol chloroform treatment and

341   ethanol precipitation. Linearized template was transcribed using MEGAscript® T7 Transcription

342   Kit (Invitrogen, Carlsbad, CA) followed by capping with NEB Vaccinia Capping System as

343   previously described [1]. To qualify the vaccine candidate *in vitro*, Baby Hamster Kidney (BHK)

344   cells (ATCC) were transfected with repRNA or mock transfected using *TransIT-mRNA*

345   transfection kit (Mirus Bio) and cells analyzed 24 hours later by immunofluorescence using a

346   mouse anti-v5 AF488 secondary antibody (Invitrogen). Additionally, BHK cells were transfected

347   with repRNA-CoV2S and repRNA-GFP and cell lysates were collected 24 hours later for analysis

348   by SDS-PAGE and by western blot using recombinant SARS-CoV-2 S protein as a positive control.

349   To detect repRNA-mediated protein expression following transfer to nitrocellulose membrane,

350   anti-v5-HRP or convalescent human serum collected 29 days after onset of PCR-confirmed

351   COVID-19 followed by anti-human Ig-HRP secondary antibody (Southern Biotech) was used.

352   ***LION formulation***. To protect the RNA replicons from degradation, we partnered them with a

353   Lipid InOrganic Nanoparticle (LION) formulation that consists of inorganic superparamagnetic

354   iron oxide (SPIO) nanoparticles within a hydrophobic squalene core to enhance formulation

355   stability. LIONs comprise 37.5 mg/ml squalene (Millipore Sigma), 37 mg/ml Span® 60 (Millipore

356   Sigma), 37 mg/ml Tween® 80 (Fisher Chemical), 30 mg/ml DOTAP chloride (Corden Pharma), 0.2

357   mg/ml 15 nm oleic acid-coated iron oxide nanoparticles (Ocean Nanotech, San Diego, CA) and

358   10 mM sodium citrate dihydrate (Fisher Chemical). LION particles were manufactured by

17

359   combining the iron oxide nanoparticles with the oil phase (Squalene, Span 60, and DOTAP) and

360   sonicating for 30 minutes in a 65°C water bath. Separately, the aqueous phase, containing

361   Tween 80 and sodium citrate dihydrate solution in water, was prepared with continuous stirring

362   until all components were dissolved. The oil and aqueous phases were then mixed and

363   emulsified using a VWR 200 homogenizer (VWR International) and the crude colloid was

364   subsequently processed by passaging through a microfluidizer at 20,000 psi with a LM10

365   microfluidizer equipped with a H10Z-100 μm ceramic interaction chamber (Microfluidics) until

366   the z-average hydrodynamic diameter – measured by dynamic light scattering (Malvern

367   Zetasizer Nano S) – reached 50 ±5 nm with a 0.2 polydispersity index. The microfluidized LION

368   was terminally filtered with a 200 nm pore-size polyethersulfone (PES) filter and stored at 2-

369   8°C.

370   **RNase protection**. Replicon RNA was complexed with LION formulations and placed on ice for

371   30 min. After diluting the complex using nuclease-free water, complexes containing 1 μg of

372   repRNA at 20 μg/mL were treated with 50 ng of RNase A (Thermo Scientific) for 30 min at room

373   temperature, followed by an incubation with 5 μg of recombinant Proteinase K (Thermo

374   Scientific) for 10 min at 55°C. RNA was then extracted using an equal volume of 25:24:1

375   phenol:chloroform:isoamyl alcohol (Invitrogen). After vortexing, samples were centrifuged at

376   17,000 × g for 15 min. The supernatant was collected and mixed 1:1 with Glyoxal load dye

377   (Invitrogen) and heated at 50°C for 15 min. The equivalent of 200 ng of RNA was loaded and run

378   on a denatured 150 mL 1% agarose gel in Northern Max Gly running buffer (Invitrogen) at 120 V

379   for 45 min. Gels were imaged using a ChemiDoc MP imaging system (BioRad). The intensity of

380   the intact RNA band was compared to phenol:chloroform:isoamyl extracted RNA from

381   complexes that were not subjected to RNase and Proteinase K treatment.

382

383   **Mouse immunizations**. All mouse experiments were conducted in accordance with procedures

384   approved by the institutional animal care and use committee. Female C57BL/6 or BALB/C mice

385   (purchased from Charles River, Wilmington, MA) were maintained in specific pathogen-free

386   conditions and entered experiments at 6-12 weeks of age unless otherwise indicated. Mice

387   were immunized by intramuscular injection of vaccine delivered in a total volume of 50 μl in the

18

388   thigh.

389

390   ***Pigtail macaque study.*** Five adult male pigtail macaques were used in these studies (aged 3-6

391   years, weight 5-13 kg). All animals received a previous Hepatitis B virus (HBV) DNA and protein

392   vaccine regimen, comprised of HBV core and surface antigens and anti-CD180 [2], and were re-

393   enrolled in this study in response to the SARS-CoV-2 pandemic. All animals were housed at the

394   Washington National Primate Research Center (WaNPRC), an accredited by the American

395   Association for the Accreditation of Laboratory Animal Care International (AAALAC), and as

396   previously described [3]. All procedures performed on the animals were with the approval of the

397   University of Washington's Institutional Animal Care and Use Committee (IACUC).

398   Blood was collected at baseline (week -2 or -1), and at days 10, 14, 28, and 42 post-

399   prime vaccination (Fig. 5A). Blood was also collected 10 days post-boost (38 days post-prime) in

400   the 50µg vaccinated animals. Serum and plasma were collected and PBMCs were isolated from

401   whole blood as previously described [4]. Animals were sedated with an intramuscular injection

402   (10 mg/kg) of ketamine (Ketaset®; Henry Schein) prior to blood collection or vaccination.

403   Animals were observed daily for general health (activity, appetite) and for evidence of

404   reactogenicity at the vaccine inoculation site (swelling, redness). They also received full physical

405   exams including temperature and weights measurements at each study timepoint. None of the

406   animals became severely ill during the course of the study and none required euthanasia.

407

408   ***Pigtail macaque immunization.*** LION and repRNA-CoV2S were complexed at a nitrogen-to-

409   phosphate molar ratio of 15 in 10mM sodium citrate and 20% sucrose buffer on ice and

410   incubated for at least 30 minutes. The 50µg vaccine was delivered intramuscularly into the

411   quadriceps muscle with one 250 µl injection on weeks 0 and 4. The 250µg vaccine was

412   delivered intramuscularly with five 250µl injections over 4 muscles, 2 in the right quadriceps, 1

413   in the left quadricep, and 1 each in the left and right deltoids on week 0. All injection sites were

414   shaved prior to injection and monitored post-injection for any signs of local reactogenicity.

415

416   ***Serum Chemistries and Complete Blood Counts.*** Serum chemistries were run on a Beckman

417   Coulter AU 680/5812 system and complete blood counts were determined on a Sysmex XN9000

418   analyzer by the University of Washington Department of Laboratory Medicine.

419

420   ***Antigen-specific antibody responses.*** Blood was collected from the retro-orbital sinus of

421   immunized mice, or venipuncture of anesthetized macaques, and serum prepared. Antigen-

422   specific IgG, IgG1, IgG2a, and IgG2c responses were detected by enzyme linked immunosorbent

423   assay (ELISA) using a previously described recombinant SARS-CoV-2 S as the capture antigen [5].

424   ELISA plates (Nunc, Rochester, NY) were coated with 1 µg/ml antigen or with serial dilutions of

425   purified polyclonal IgG from mouse our monkeys to generate a standard curve in 0.1 M PBS

426   buffer and blocked with 0.2% BSA-PBS. Then, in consecutive order, washes in PBS/Tween,

427   serially diluted serum samples, anti-mouse or-monkey IgG, IgG1, IgG2a, or IgG2c-HRP (Southern

428   Biotech, Birmingham, AL) and TMB then HCL were added to the plates. Plates were analyzed at

429   405nm (EL$_X$808, Bio-Tek Instruments Inc, Winooski, VT). Absorbance values from the linear

430   segment of each serum dilution curve was used to interpolate the standard curve and calculate

431   the IgG concentration present in each sample.

432

433   ***SARS-CoV-2 pseudovirus neutralization.*** Murine leukemia virus (MLV)-based SARS-CoV-2 S-

434   pseudotyped viruses were prepared as previously described [5,6]. In brief, HEK293T cells were co-

435   transfected with a SARS-CoV-2 (based on Wuhan-Hu-1 isolate) S-encoding plasmid, an MLV

436   Gag-Pol packaging construct, and the MLV transfer vector encoding a luciferase reporter using

437   the Lipofectamine 2000 transfection reagent (Life Technologies) according to the

438   manufacturer's instructions. Cells were incubated for 5 hours at 37°C with 8% CO2 with DNA,

439   lipofectamine, and OPTIMEM transfection medium. Following incubation DMEM containing

440   10% FBS was added for 72 hours. Pseudovirus was then concentrated using a 30kDa Amicon

441   concentrator for 10 minutes at 3,000 x g and frozen at -80C.

442   BHK cells were plated in 96 well plates for 16-24 hours prior to being transfected with

443   human ACE2 using standard lipofectamine 2000 protocol and incubated for 5 hours at 37°C

444   with 8% CO2 with DNA, lipofectamine, and OPTIMEM transfection medium. Following

445   incubation, DMEM containing 20% FBS was added in equal volume to the OPTIMEM

446   transfection media for 16-24 hours. Concentrated pseudovirus with or without serial dilution of

447   antibodies was incubated for 1 hour at room temperature and then added to the wells after

448   washing 3X with DMEM and removing all media. After 2-3 hours, equal volumes of DMEM

449   containing 20% FBS and 2% PenStrep was added to the cells for 48 hours. Following 48 hours of

450   infection, equal volume of One-Glo-EX (Promega) was added to the cells and incubated in the

451   dark for 5-10 minutes prior to reading on a Varioskan LUX plate reader (ThermoFisher).

452   Measurements were done in duplicate and relative luciferase units (RLU) were recorded.

453

454   ***SARS-CoV-2 neutralization.*** Three-fold (pigtail macaque) or four-fold (human) serial dilutions of

455   heat inactivated serum and 600 plaque-forming units (PFU)/ml solution of SARS-CoV-2/WA/20

456   (BEI resources) were mixed 1:1 in DPBS (Fisher Scientific) + 0.3% gelatin (Sigma G7041) and

457   incubated for 30 min at 37°C. Serum/virus mixtures were added in duplicate, along with virus

458   only and mock controls, to Vero E6 cells (ATCC) in a 12-well plate and incubated for 1hr at 37°C.

459   Following adsorption, plates were washed once with DPBS and overlayed with a 1:1 mixture of

460   Avicel RC-591 (FMC) + 2 x MEM (ThermoFisher) supplemented with 4% heat-inactivated FBS

461   and Penicillin/Streptomycin (Fisher Scientific). Plates were then incubated for 2 days at 37°C.

462   Following incubation, overlay was removed and plates were washed once with DPBS and then

463   10% formaldehyde (Sigma-Aldrich) in DPBS was added to cells and incubated for 30 minutes at

464   room temp. Plates were washed again with DPBS and stained with 1% crystal violet (Sigma-

465   Aldrich) in 20% EtOH (Fisher Scientific). Plaques were enumerated and percent neutralization

466   was calculated relative to the virus-only control.

467

468   ***Mouse IFN-γ ELISPOT.*** Spleen and lung lymphocytes were isolated from mice 12 days after the

469   second vaccination. MIAPS4510-Multiscreen plates (Millipore) were coated with rat anti mouse

470   IFN-gamma capture antibody (BD) in PBS and incubated overnight at 4°C. The plates were

471   washed in PBS and then blocked (2h, RT) with RPMI medium (Invitrogen) containing 10% heat

472   inactivated fetal calf serum (Gibco). Lung and spleen cells were plated at $5x10^5$ and $2.5x10^5$

473   cells/well and stimulated with the SARS-Cov2 S peptide pools (11aa overlapping 15 mer

474   peptides from Genscript) at 1.5 μg/ml/peptide and cultured for 20 hours (37°C, 5% CO_2).

475   Biotinylated anti-mouse IFN-gamma antibody (BD) and streptavidin-Alkaline Phosphotase-

476   substrate (Biolegend) were used to detect IFN-gamma secreting cells. Spot forming cells were

477   enumerated using an Immunospot Analyzer from CTL Immunospot profession software

478   (Cellular Technology Ltd).

479

480   ***Statistical analyses.*** Statistical analyses were conducted in Prism (Graphpad) using one-way

481   analysis of variance and Tukey's multiple comparison test used to compare more than two

482   groups, and either student's t or Mann Whitney U tests to compare two groups. Statistical

483   significance was considered when the p-values were < 0.05.

484   ***Data availability.*** Data have been deposited in Figshare: 10.6084/m9.figshare.12385574
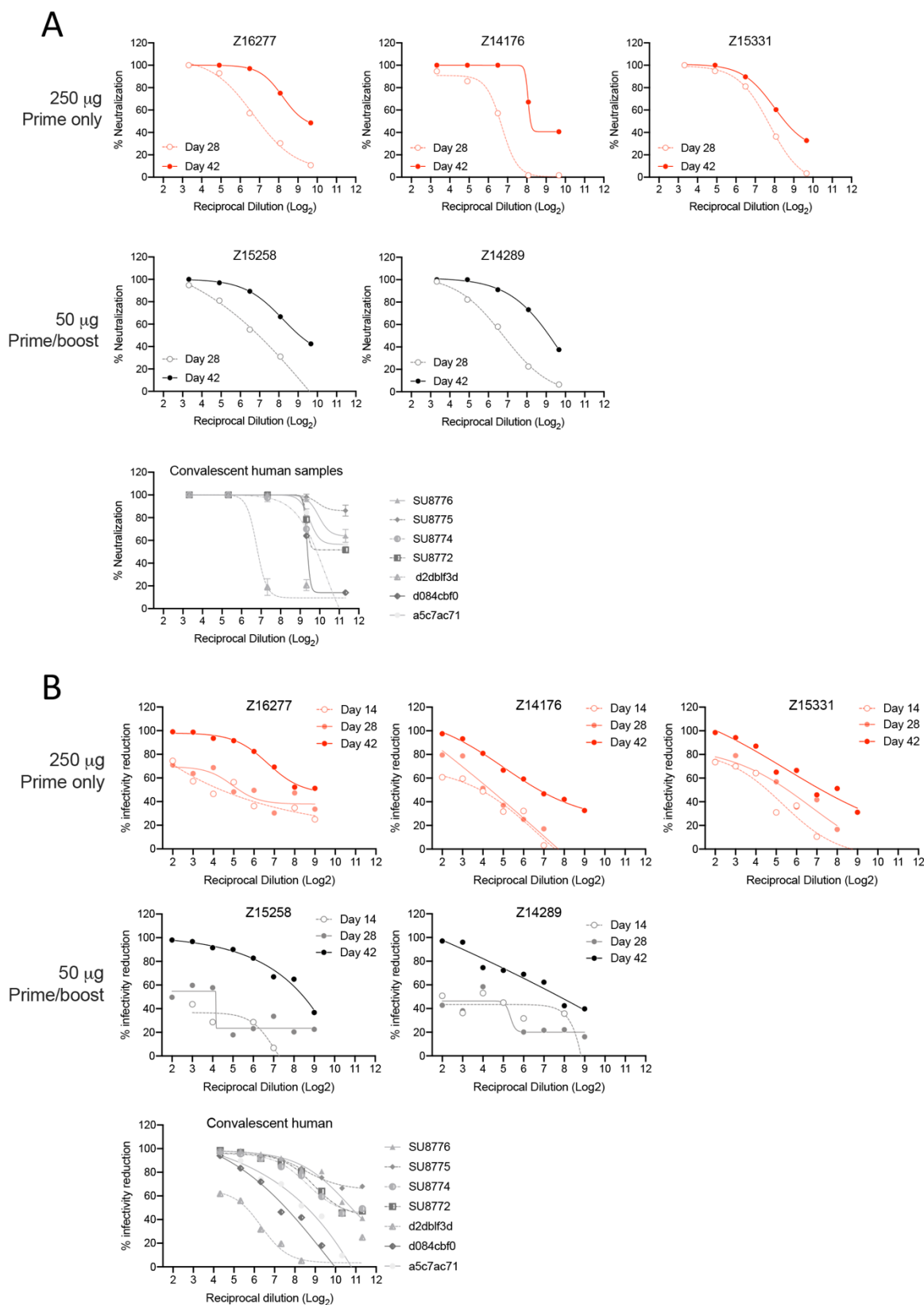
Supplemental Figures
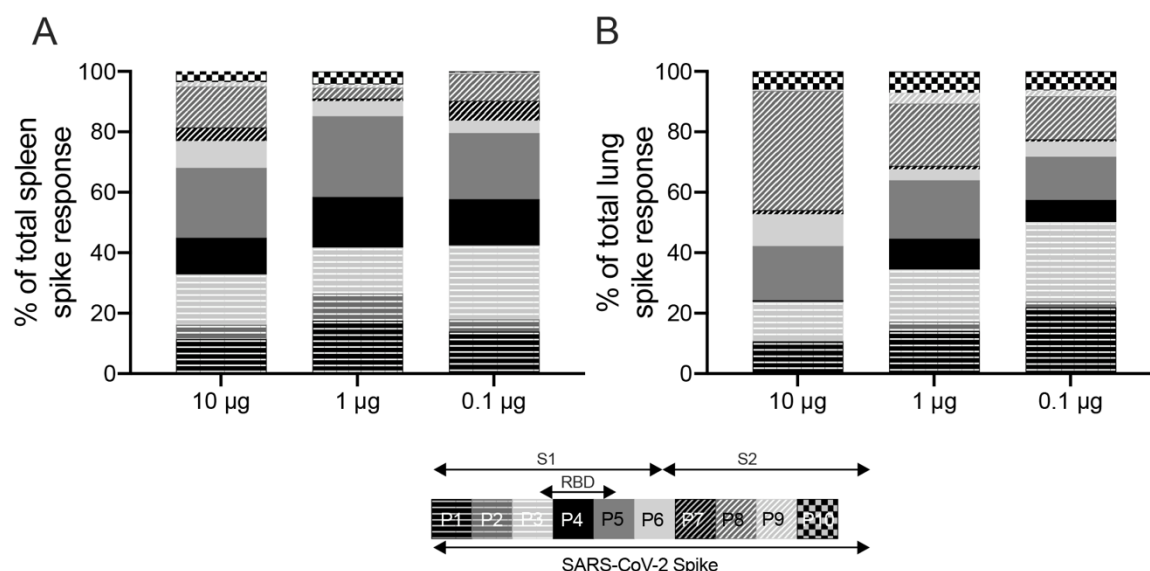
Supplemental Figure 1. Breadth of T-cell responses in C57BL/6 mice. Six to eight-week old C57BL/6 mice (n=5/group) received 10, 1, or 0.1 μg LION/repRNA-CoV2S via the intramuscular route. On day 28, mice received a booster immunization and 12 days later, (**A**) spleens and (**B**) lungs were harvested and IFN-γ responses were measured by enzyme-linked immune absorbent spot (ELISpot) following stimulation with 10 peptide pools encompassing the entire Spike protein. Each peptide pool consisted of 26-29 15-mer peptides overlapping by 11 amino acids. Data are presented as percent of total spike response.
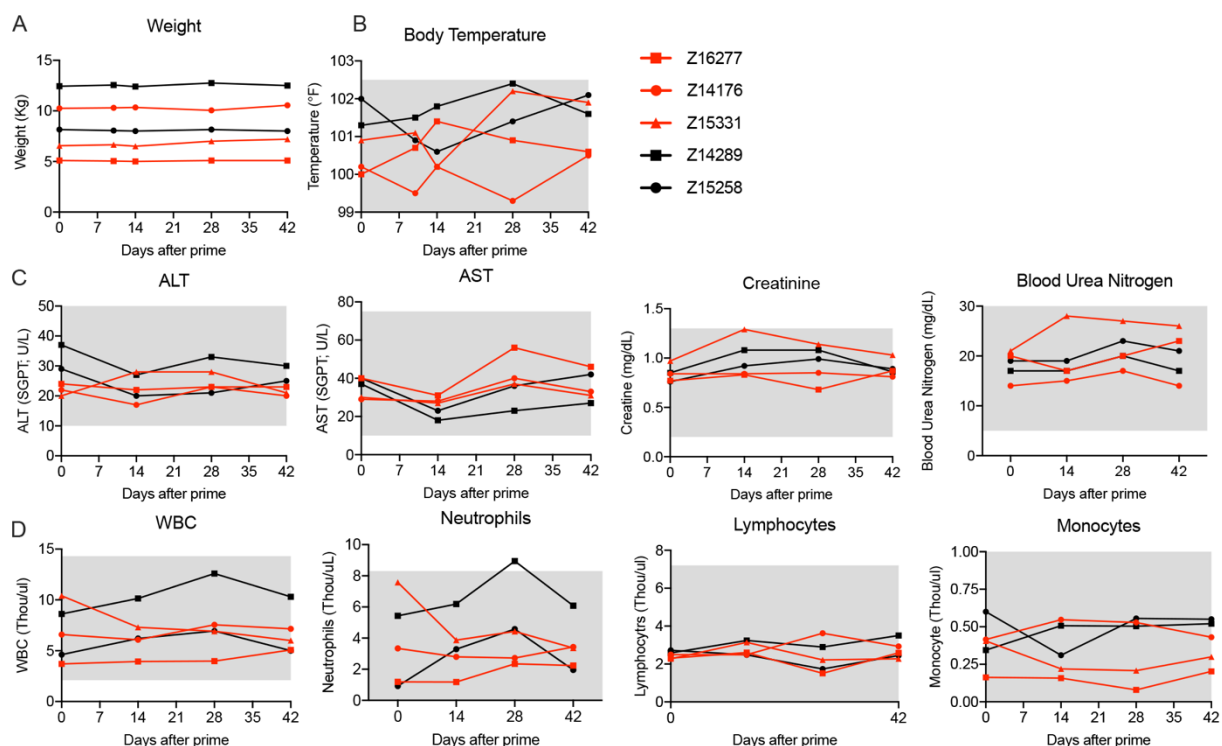
Supplemental Figure 2. **Vaccination did not induce adverse reactions in pigtail macaques.** (**A**). Body weight in kg. (**B**) Rectal body temperature in Fahrenheit. (**C**) Serum chemistries. (**D**) Blood complete blood counts (CBC). (**A-D**) Grey shaded areas indicate normal ranges for pigtail macaques.

487
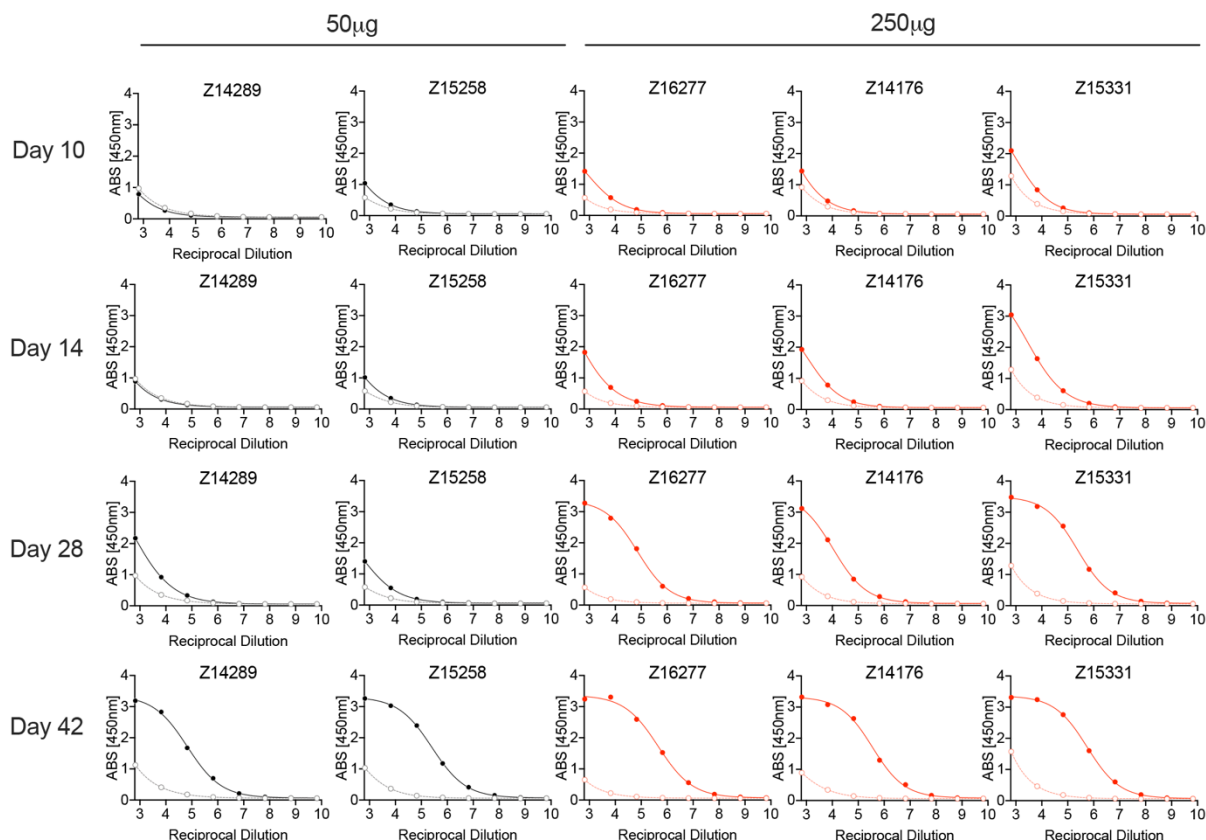
Supplemental Figure 3. Raw ELISA absorbance values from pigtail macaque study. Recombinant SARS-CoV-2, based on the Wuhan-Hu-1 isolate, was used as the capture antigen and goat anti-monkey IgG-HRP used as the secondary conjugate. Absorbance values were determined at 405nm. Data are presented as pre-immune sera (open circles, dotted line) with post-immune sera (closed circles, solid line). Data are presented as pre-immune sera (open circles, dotted line) with post-immune sera (closed circles, solid line).

488

Supplemental Figure 4. Neutralization curves of pigtail macaque and human samples against (A) SARS-CoV-2/WA/2020 or (B) pseudotyped virus. SARS-CoV-2/WA/2020 neutralization was performed on sera collected from macaques on days 28 and 42 post-primary immunization. Pseudoviral (SARS-CoV-2 Wuhan-Hu-1 pseudotype) neutralization was performed on sera collected from macaques on days 14, 28, and 42 post-primary. (see Sup. Table 1). Both assays were performed alongside sera from 7 convalescent humans collected at various timepoints after their first positive test for SARS-CoV-2 infection.

489

Supplemental Table 1. Convalescent sera from COVID-19 patients

Sample ID	Days post onset	PRNT$_{80}$
SU8776	20	1119
SU8775	15	<20
SU8774	21	496
SU8772	unknown	635
d2db1f3d	35	88
d084cbf0	29	607
a5c7ac71	64	658

490

Supplemental References

1. Erasmus, J. H. *et al.* A Nanostructured Lipid Carrier for Delivery of a Replicating Viral RNA Provides Single, Low-Dose Protection against Zika. *Mol. Ther.* **26**, 2507–2522 (2018).

2. Chaplin, J. W., Chappell, C. P. & Clark, E. A. Targeting antigens to CD180 rapidly induces antigen-specific IgG, affinity maturation, and immunological memory. *J. Exp. Med.* **210**, 2135–2146 (2013).

3. Munson, P. *et al.* Therapeutic conserved elements (CE) DNA vaccine induces strong T-cell responses against highly conserved viral sequences during simian-human immunodeficiency virus infection. *Hum. Vaccin. Immunother.* **14**, 1820–1831 (2018).

4. O'Connor, M. A. *et al.* Mucosal T Helper 17 and T Regulatory Cell Homeostasis Correlate with Acute Simian Immunodeficiency Virus Viremia and Responsiveness to Antiretroviral Therapy in Macaques. *AIDS Res. Hum. Retroviruses* **35**, 295–305 (2019).

5. Walls, A. C. *et al.* Structure, function and antigenicity of the SARS-CoV-2 spike glycoprotein. *bioRxiv* 2020.02.19.956581 (2020) doi:10.1101/2020.02.19.956581.

6. Millet, J. K. & Whittaker, G. R. Murine Leukemia Virus (MLV)-based Coronavirus Spike-pseudotyped Particle Production and Infection. *Bio-protocol* **6**, e2035 (2016).